Theor Chem Acc (2015) 134:101
DOI 10.1007/s00214-015-1702-y

REGULAR ARTICLE

Development of an AMOEBA water model using GEM distributed multipoles

Hedieh Torabifard[1] · Oleg N. Starovoytov[2] · Pengyu Ren[3] · G. Andrés Cisneros[1]

Received: 29 June 2015 / Accepted: 15 July 2015 / Published online: 2 August 2015

Abstract Distributed multipoles obtained from the Gaussian electrostatic model (GEM) have been previously shown to be amenable for use in the AMOEBA force field [JCTC(2012) 12, 5072]. GEM distributed multipoles (GEM-DM) were determined for several systems including water. This previous AMOEBA water model with GEM-DM included only monopoles on the hydrogens and multipoles up to quadrupoles on the oxygen. This model showed good agreement with experiment for several properties at room temperature, but not at higher temperatures. In this contribution, we present the development of an AMOEBA water model using GEM-DM with distributed multipoles for each atomic site up to the quadrupole level. Quantum mechanical energy decomposition analysis has been employed to compare each term of the force field for parametrization. The inclusion of higher-order multipoles on hydrogen atoms is shown to provide better agreement with experiment on a number of properties including liquid density (ρ), enthalpy of vaporization (ΔH_{vap}), heat capacity (C_p), and self-diffusion coefficient (D) for a range of temperatures.

Keywords AMOEBA · Distributed multipoles · Polarizable force field · Water model

✉ G. Andrés Cisneros
andres@chem.wayne.edu

[1] Department of Chemistry, Wayne State University, Detroit, MI 48202, USA

[2] Department of Physics, University of Houston, Houston, TX 77204, USA

[3] Department of Biomedical Engineering, The University of Texas at Austin, Austin, TX 78712, USA

1 Introduction

Water is arguably the most important and interesting liquid on earth. It has many interesting physical and chemical properties largely due to the ability of water molecules to form multiple hydrogen bonds. Unique properties such as the temperature of maximum density, large heat capacity, expansion on freezing, and unique solvation properties make water very important in several areas including biology and geology. The manner in which water interacts with ions, organic molecules, and biomolecules holds the key for many questions about the foundation of biomolecular structure and function.

The investigation of microscopic properties of liquid water remains a subject of intense research [15, 38–40, 53–55]. Several theoretical and computational models have been developed to attempt to describe the detailed microscopic properties of water. These models can be useful tools to guide and supplement experimental work [22, 35, 41, 49].

There are many non-polarizable and polarizable water models as has been reviewed extensively previously [24, 63]. Some of these potentials are very popular in computational studies; for instance, point charge-based TIP3P water model is widely used for biomolecular simulations [28]. This model was parameterized to reproduce a number of properties at ambient conditions, including heat of vaporization, liquid density, and isobaric heat capacity at 298 K [63]. However, this model has been shown to fail to reproduce thermodynamic properties at elevated temperatures [30, 64, 65]. Improvements based on TIP3P have been developed in several improved models such as TIP4P and TIP4P-Ew [63].

One of the main reasons for the issues observed from these simple models involves the reduced accuracy of the non-bonded interactions. This reduced accuracy arises

from several factors, including the inaccurate representation of the charge density anisotropy, the failure to account for penetration effects [59], and the neglect of many-body interactions [5]. There are several ways to address these shortcomings; for instance, the error due to charge density anisotropy can be reduced by using higher-order multipoles; however, these models do not account for penetration errors [21, 59]. The penetration effect may be accounted by the use of damping functions at close distances [14, 21, 29, 43, 60, 66].

In addition, various explicit polarization models have been introduced to account for the change in the charge distribution due to an external electric field [26, 52]. The inclusion of polarizabilities also results in (partial) accounting of many-body effects [60]. For instance, the POL3 model [9] is an atomic polarizable water model that employs undamped isotropic dipoles [8]. Some polarizable models such as AMOEBA [44], SIBFA [23], EFP [17], XPOL [69, 70], and NEMO [27] rely on distributed multipoles and explicit polarization for the electrostatic component of the non-bonded interactions. The improved description of the charge density anisotropy results in an improved reproduction of the electrostatic interactions due to the use of distributed multipoles [32, 45–47, 59]. One of the most accurate current models to describe water is the MB-pol potential developed by Babin et al. [3, 4]. MB-pol relies on the many-body expansion at medium and short range combined with a multipolar polarizable description at long range and inclusion of nuclear quantum effects [3, 4]. MB-Pol is able to reproduce structural, thermodynamic, and dynamical properties of the liquid phase as well as dimer vibration–rotation tunneling spectrum, second and third virial coefficients, and cluster structures and energies in the gas phase [36].

AMOEBA is a multipolar polarizable potential that relies on distributed atomic multipoles up to the quadrupole and inducible point dipoles. The original AMOEBA water model, referred to as AMOEBA03 herein [49, 50], employs mutual induction of dipoles at atomic centers for the reproduction of the polarization component. AMOEBA03 also employs a Tholè damping function to avoid the so-called polarization catastrophe [61] at short range. This potential showed improvement in the description of several gas-phase properties of water, which was attributed to the use of multipole moments beyond the monopoles [68]. The AMOEBA03 model also shows good agreement with various thermodynamic properties compared to experiment [49].

A scaled-down version of the AMOEBA water model, termed iAMOEBA (inexpensive AMOEBA) [68], was introduced in 2013. The computational cost is reduced by a factor of two by implementing a method of direct polarization [68], that is, in iAMOEBA only the electric fields that arise from the permanent multipoles are taken into account for the calculation of the polarization. The distinctive feature of iAMOEBA compared with AMOEBA03 is the use of ForceBalance for its parametrization [67]. Parametrization by means of ForceBalance involves the use of an objective minimization procedure to optimize the fitting parameters by combining gas-phase quantum data and computed thermodynamic properties [68]. A large and diverse data set with different weights and scaling factors such as experimental liquid properties and ab initio quantum mechanics (QM) gas-phase dimer results are used to optimize the parameters. We have recently developed a similar method for optimization of vdW parameters by fitting the dimer energies, density, and heat of vaporization to ab initio and experimental data [7]. Recently, a new AMOEBA water model has been introduced, which also relied on the ForceBalance approach (AMOEBA14) [33]. AMOEBA14 showed significant improvement over both AMOEBA03 and iAMOEBA for a number of liquid properties across a range of temperatures and pressures, as well as gas-phase properties.

An alternative way to improve the accuracy of the electrostatic interactions is to employ a continuous description of the charge density. One method that relies on this approach is the Gaussian electrostatic model (GEM) [12, 13, 18, 42], which uses Hermite Gaussian functions to describe the molecular charge density. An added advantage of the fitting proceduer for GEM is that it enables the calculation of explicitly finite distributed multipoles (GEM-DM) [13]. These multipoles have been employed to describe the electrostatic interactions in the AMOEBA potential [11, 56].

The original AMOEBA parametrization with GEM-DM was focused on several systems including liquid water. The electronic density for this water model was fitted by employing a basis set that included Gaussian Hermite functions up to $l = 2$ for the oxygen and $l = 0$ (only s-type functions) on the hydrogen atoms [11]. Therefore, the final distributed multipoles for the water model involve monopoles, dipoles, and quadrupoles on the oxygens and only monopoles on the hydrogen atoms. This initial AMOEBA model with GEM-DM showed very good agreement for liquid structure, density, and heat of vaporization compared with experimental data at 298 K. However, it failed to predict the temperature of maximum density of water.

In this study, we report the parametrization of a new AMOEBA water model using GEM-DM by considering moments up to quadrupoles on both oxygen and hydrogen atoms. The multipoles, which are fitted to QM data, describe the electrostatic interaction very well at long and medium range. The van der Waals parameters are fitted to experimental density and heat of vaporization at ambient condition. The accuracy of the AMOEBA/GEM-DM force field is tested by running a series of simulations

and comparing thermodynamic and transport properties to results from a published benchmark of water properties reported by Vega et al. [63]. The calculated results are shown to reproduce liquid- and gas-phase properties very well for a broad range of temperatures including the temperature of the maximum density of water as well as other thermodynamic and transport properties. The remainder of the paper is organized as follows: In Sect. 2, we describe the methodology for the parametrization of the force field and the details of the molecular dynamics simulations. In Sect. 3, the results for parametrization and simulation are discussed, followed by concluding remarks.

2 Computational methods

The parametrization details employed in the present study have been described in detail in previous papers [11, 56]. A brief explanation of the parameter fitting methodology is presented in Sect. 2.1, followed by a description of the MD simulation setup in Sect. 2.2.

2.1 Parametrization details

AMOEBA potential including five bonded and three non-bonded terms is shown in Eq. 1 [44].

$$U_{\text{total}} = U_{\text{bond}} + U_{\text{angle}} + U_{b\theta} + U_{\text{out}} + U_{\text{torsions}} + U_{\text{Coul}} + U_{\text{Pol}} + U_{\text{vdw}} \quad (1)$$

As explained previously [11, 56], the bonded terms are taken directly from AMOEBA without any adjustment [48, 49, 51]. In the case of the non-bonded terms, described by the last three terms of the potential (see Eq. 1): U_{Coul}, U_{Pol}, and U_{vdw}, all parameters have been fitted to reproduce results based on QM energy decomposition analysis (EDA) for the Coulomb and Polarization terms. For the van der Waals term, the initial parameters were fitted to reproduce the gas-phase EDA results and subsequently refined against two experimental data points (see below).

Total intermolecular energies were calculated using the counterpoise correction to take into account the basis set superposition error (BSSE) [57] at the MP2/aug-cc-pVTZ level as a function of intermolecular separation for the canonical water dimer. The intermolecular polarization interactions for each pair were calculated using the restricted variational space (RVS) decomposition approach [31] at the HF/aug-cc-pVTZ level of theory as implemented in GAMESS [6]. An in-house FORTRAN90 program that uses ab initio monomer densities was employed to calculate the Coulomb intermolecular energies for each dimer. Finally, the van der Waals energies were obtained by subtracting the Coulomb and polarization energies from total intermolecular energy for each dimer, as described in Eq. 2:

$$U_{\text{vdw(MP2-HF)}} = U_{\text{Tot(MP2)}} - (U_{\text{Coul(MP2)}} + U_{\text{Pol(HF)}}) \quad (2)$$

GEM distributed multipoles (GEM-DM) up to quadrupoles on each atom were obtained using the GEM-fit program [11]. The Hermite coefficients and associated distributed multipoles were calculated by fitting the relaxed one-electron density from a single water molecule (in the AMOEBA optimized geometry) calculated at the MP2/aug-cc-pVTZ level and fitted using the A2 [2] auxiliary basis set.

These distributed multipoles are used to determine the intermolecular Coulomb interactions by

$$U_{\text{Coul}}(r_{ij}) = M_i^T T_{ij} M j, \quad (3)$$

where T_{ij} is a multipole interaction matrix, M is a polytensor which represents the multipole components, and r_{ij} is the distance between site i and site j.

In our previous work [11], multipole moments were calculated using the A1 ABS, which contains only s-type functions on the hydrogen atoms. This results in only monopole components available on the hydrogen atoms. As described above, the results obtained with this model showed good agreement with QM reference data for intermolecular interactions and with experimental values for thermodynamic properties at 298 K. However, this model was not able to describe the behavior of system at elevated temperatures. In the current water model, we have employed the same reference electronic density as in our original model, except that the A2 auxiliary fitting basis set was employed. This ABS includes higher-order angular momentum functions ($l = 2$) on the hydrogen atoms [11]. The old and new multipoles are compared in Table 1.

The polarization term is described by inducible atomic dipoles on each interaction (atomic) site. Here, each induced dipole is obtained by $\mu_{i,\alpha}^{\text{ind}} = \alpha_i E_{i,\alpha}$, where α is the atomic polarizability, and $E_{i,\alpha}$ is the external electric field generated by both permanent multipoles and induced dipoles. The Tholé damping function [58, 62] is employed to avoid the "polarization catastrophe" at short range. In our previous study, the Tholé parameter was reduced to 0.35 to get a better description of the polarization interactions for the canonical water dimer [11]. In the current work, the damping factor was set to 0.39 (consistent with AMOEBA03) and resulted in good agreement for the polarization contribution (see below).

The last term is the van der Waals potential energy, which is described by the buffered Halgren [25] pairwise potential (see Eq. 4)

$$U_{\text{vdw}}(r_{ij}) = \epsilon_{ij} \left(\frac{1 + 0.07}{\left(\frac{r_{ij}}{R_{ij}^0}\right) + 0.07} \right)^7 \left(\frac{1 + 0.12}{\left(\frac{r_{ij}}{R_{ij}^0}\right)^7 + 0.12} - 2 \right), \quad (4)$$

Table 1 Comparison of multipoles using A1 and A2 ABSes for water

ABS	Atoms	Multipoles		
A1	Oxygen	−0.92473		
		0.00192	−0.00015	−0.27413
		0.49614		
		0.00067	−0.36190	
		0.00182	0.00041	−0.13424
	Hydrogen	0.46237		
		0.00000	0.00000	0.00000
		0.00000		
		0.00000	0.00000	
		0.00000	0.00000	0.00000
A2	Oxygen	−0.41444		
		0.00000	0.00000	0.01503
		0.61476		
		0.00000	−0.49728	
		0.00000	0.00000	−0.11748
	Hydrogen	0.20722		
		−0.00600	0.00000	−0.21386
		0.05872		
		0.00000	0.04492	
		0.00216	0.00000	−0.10365

where ϵ_{ij} is the potential well, r_{ij} is the separation distance between sites i and j, and R^0_{ij} is the minimum energy interaction distance for sites i and j. The van der Waals parameters for molecules are calculated using the Lorentz–Berthelot combining rule [44].

$$\sigma_{ij} = \frac{1}{2}(\sigma_{ii} + \sigma jj) \tag{5}$$

$$\epsilon_{ij} = \sqrt{\epsilon_{ii}\epsilon jj} \tag{6}$$

Validation of the new parameters was performed by running a series of molecular dynamics simulations for liquid and gas phases and comparing the resulting calculated properties with experimental data and other molecular dynamics simulation results.

2.2 MD simulation

MD simulations were carried out using the AMOEBA/GEM-DM force field in the AMBER12 [10] simulation package. The MD simulations were performed using a cubic simulation cell with periodic boundary conditions. The calculated system included 216 water molecules (648 atoms). Simulations were carried out in the NPT ensemble with an integration time step of 1 fs. Long-range electrostatic effects were computed employing the smooth particle mesh Ewald method [16, 20, 37] with an 8 Å direct cutoff. Sampling trajectories were generated for 4 ns.

3 Results

This section presents the parametrization procedure, and results are obtained for the new AMOEBA/GEM-DM water model. Section 3.1.1 presents the results for the parametrization calculations for the intermolecular parameters. This is followed by the results for the parametrization of the van der Waals term in Sect. 3.1.2, and the validation of the water model by calculating various thermodynamic and transport properties as discussed in Sect. 3.2.

3.1 Force field parametrization

3.1.1 Intermolecular interactions

A series of water dimers was generated by systematically varying the distance (increments of 0.1 Å) between the center of mass of the oxygen atom in one monomer with respect to the hydrogen atom in another monomer to calculate intermolecular interaction energies for the canonical water pair (Fig. 1). The total interaction energy for these dimers in the gas phase was calculated at the MP2(full)/aug-ccpVTZ level of theory using BSSE in Gaussian09. For these dimers, the minimum interaction distance is located at 2 Å with a corresponding intermolecular interaction energy of −4.71 kcal/mol compared with −4.69 using AMOEBA/GEM-DM. The complete intermolecular potential energy surface is shown in Fig. 2.

Next, we performed EDA to compare the intermolecular energies due to Coulomb, polarization, and Van der Waals interactions as a function of separation distance with the reference *ab initio* calculations. Intermolecular Coulomb interactions and polarization interactions are shown in Fig. 3. Intermolecular electrostatic interactions are well described at medium and long range, and a deviation at short intermolecular distances is observed, which is due to penetration errors. The van der Waals parameters were taken directly from the AMOEBA force field (see Fig. 2).

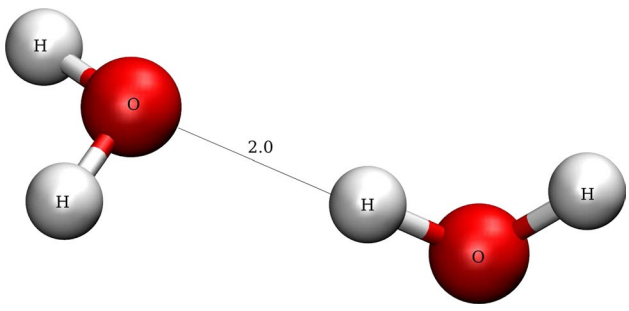

Fig. 1 Distance between the center of mass of the oxygen atom in one monomer with respect to the hydrogen atom in another monomer in Å

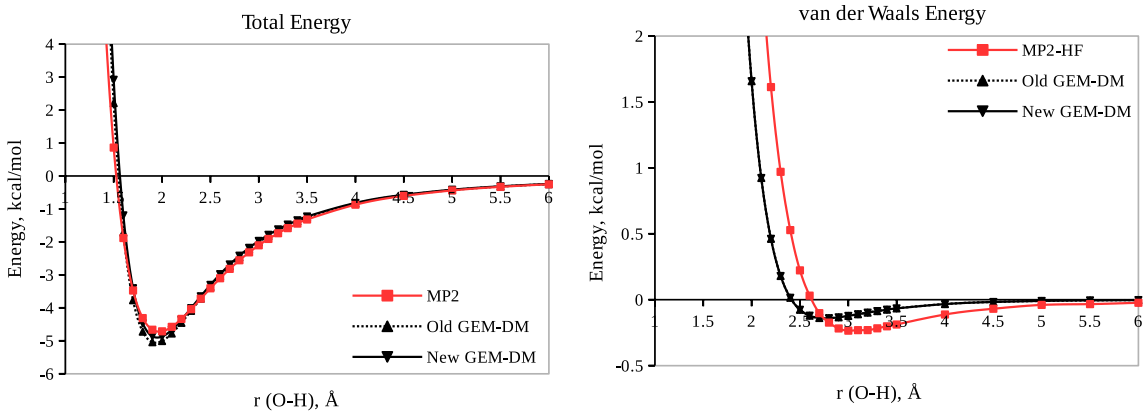

Fig. 2 Total interaction energy and vdW interactions for water dimers

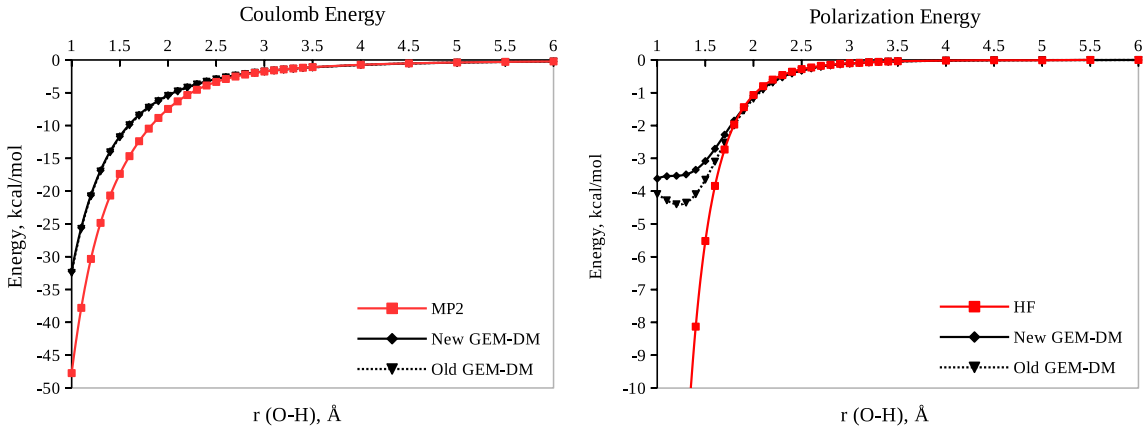

Fig. 3 Intermolecular Coulomb interactions and polarization interactions for water dimers

Table 2 Van der Waals parameter, density, and heat of vaporization before and after scaling the vdW parameters

Atoms	R	ϵ	ρ	ΔH_{vap}
A				
O	3.405	0.1100	1.062	11.22
H	2.655	0.0135		
B				
O	3.480	0.1077	1.005	10.53
H	2.680	0.0113		

A Before fitting the vdW parameters, *B* After fitting the vdW parameters. Densities are in g cm^{-3} and heat of vaporizations are in kcal mol^{-1}

Reference van der Waals energies were calculated as the difference between total intermolecular energies at the MP2 level and the Coulomb energies due to permanent multipoles, and the energies due to the polarization interaction as described in Eq. 4.

3.1.2 Van der Waals parameter fitting

As explained above, we used the original AMOEBA van der Waals parameters as a starting point for the parametrization. Our simulation results showed that the liquid density and heat of vaporization at 298 K were overestimated ($\rho = 1.062$ g cm^{-3}, $\Delta H_{gap} = 11.22$ kcal mol^{-1}) compared to the experimental data ($\rho = 0.997$ g cm^{-3}, $\Delta H_{vap} = 10.51$ kcal mol^{-1}) [63]. Therefore, we optimized these parameters initially to fit to the QM data in Fig. 2 and subsequently refined them to match the experimental density and heat of vaporization at this single temperature.

The fitted van der Waals parameters are shown in Table 2. The vdW and total intermolecular energy for a series of water dimers show excellent agreement after fitting the vdW parameters (see Fig. 4). After scaling of the van der Waals parameters, MD simulations were carried out to calculate other thermodynamic and transport properties to validate these new parameters (see Sect. 3.2).

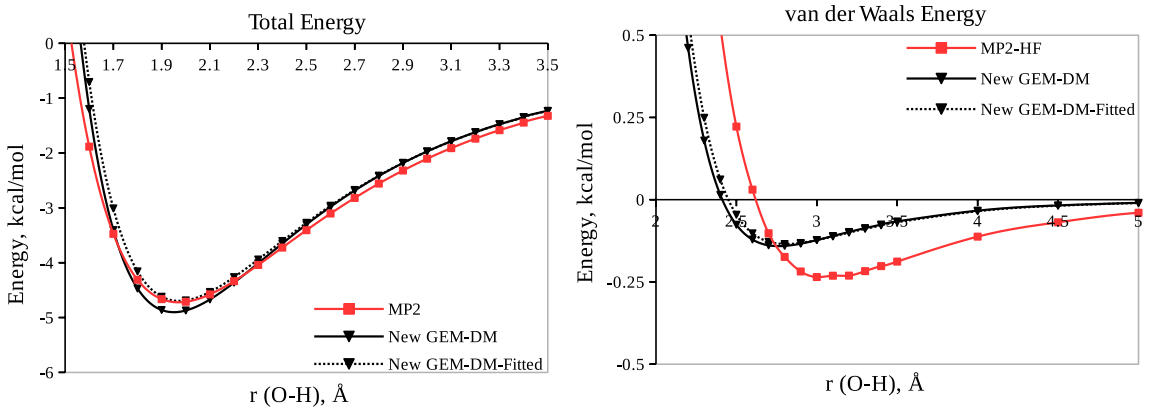

Fig. 4 Total interaction energy and vdW interactions for water dimers

3.2 Simulation results

Molecular dynamics simulations were performed to validate the accuracy of the newly developed AMOEBA parameters. This section presents the results obtained for the calculation of a series of thermodynamic and structural properties including liquid densities, heat of vaporization, heat capacity, diffusion coefficients, and liquid structure (from radial distribution functions).

3.2.1 Liquid volume and density

The calculated volume is 29.76 Å^3 at T = 298 K based on the average density from the MD simulations. Using the original van der Waals parameters, the liquid density is 6.5 % higher than the experimental value at 298 K. In contrast, after the van der Waals parameters were scaled, the liquid density decreases to 1.005 g cm^{-3} which is in good agreement with the experimental result, with an error of 0.8 % as shown in Table 2. Liquid densities calculated with AMOEBA14 and AMOEBA03 at 298.15 K are 0.998 and 1.000 g cm^{-3} respectively [33]. Comparison of the MD simulation results with experiment for liquid densities in the range of 250–370 K is shown in Fig. 5. Both MD simulation results and experiment show a maximum density at 280 K with a value of 1.007 and 1.000 g cm^{-3}, respectively (Fig. 5). The mean absolute deviation (MAD) from experiment for liquid densities calculated across all temperatures (250–370 K) is 0.006 g cm^{-3} (see Table 3), which is slightly higher than the MAD value obtained with AMOEBA14 (0.001 g cm^{-3}) [33].

3.2.2 Enthalpy of vaporization

The enthalpy of vaporization is calculated as an estimation of the strength of intermolecular interactions for water molecules. We used the following equation with the assumption of ideal gas behavior to calculate the heat of vaporization.

$$\Delta H_{\text{vap}} = \langle U_{\text{gas}} \rangle - \frac{\langle U_{\text{tot}}^{\text{liq}} \rangle}{N} + RT, \tag{7}$$

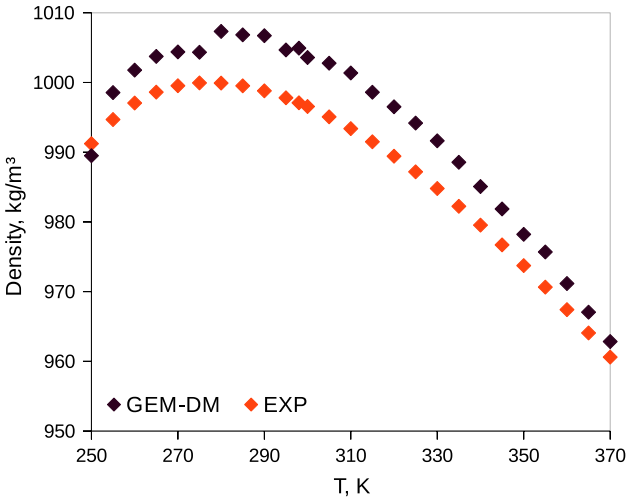

Fig. 5 Comparison of simulation results for water density with experiment between 250 and 370 K

Table 3 Mean absolute deviation (MAD) from experimental liquid-phase properties calculated by AMOEBA/GEM-DM and AMOEBA14

Property	AMOEBA/GEM-DM	AMOEBA14	Units
ρ	0.006	0.001	g cm^{-3}
ΔH_{vap}	−0.005	0.103	kcal mol^{-1}
C_p	1.54	2.28	cal mol^{-1} K^{-1}

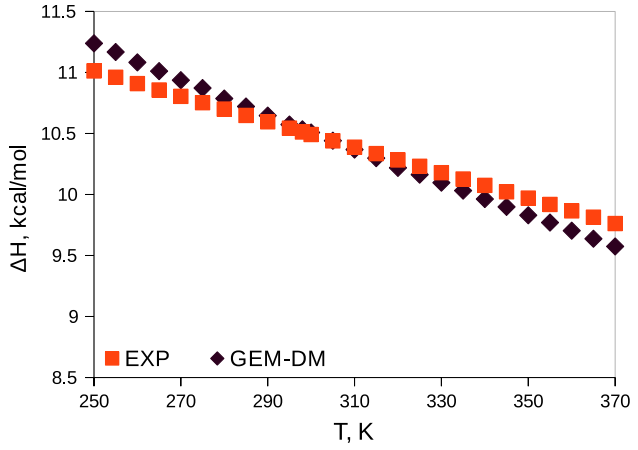

Fig. 6 Comparison of simulation results for heat of vaporization of water with experiment between 250 and 370 K

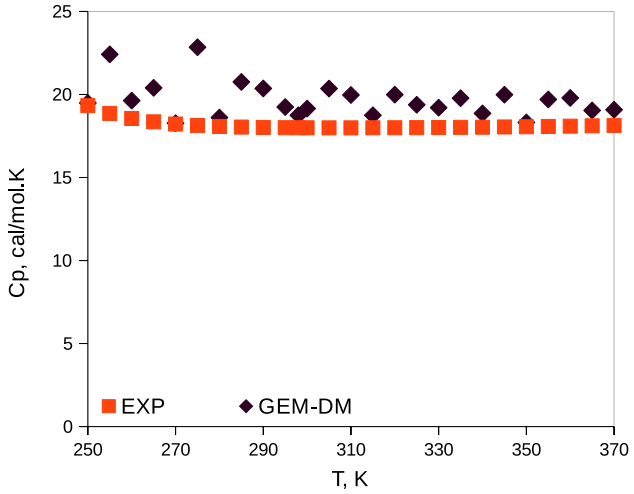

Fig. 7 Comparison of simulation results for water isobaric heat capacity with experiment between 250 and 370 K

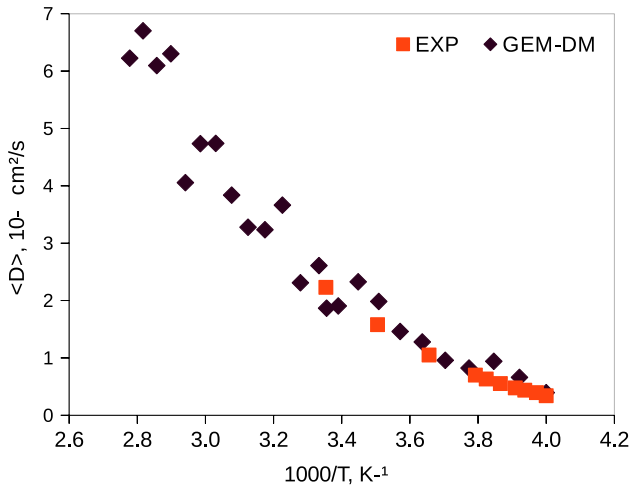

Fig. 8 Comparison of simulation results for water diffusion coefficient with experiment between 250 and 370 K

where the gas-phase energy for a single water molecule at 298 K is calculated using stochastic molecular dynamics simulations ($E_{\text{gas}} = 0.91$ kcal mol^{-1}). The calculated enthalpy of vaporization for water with GEM-DM is 10.53 kcal mol^{-1}, which is 2 % higher than the experiment value of 10.51 kcal mol^{-1} at 298 K. By comparison, the results obtained with iAMOEBA (10.94 kcal mol^{-1}) and AMOEBA14 (10.63 kcal mol^{-1}) are slightly higher than the experimental result [33, 68].

The heat of vaporization was also calculated outside of ambient conditions and compared to experimental data (Fig. 6). The MAD from experiment for heat of vaporization is 0.005 kcal mol^{-1} (See Table 3).

3.2.3 Heat capacity

The constant-pressure-specific heat capacity is $c_p = (\frac{\delta H}{\delta T})_p$. By using $\langle H \rangle = \langle E_{\text{tot}} \rangle + \langle PV \rangle$, in which PV is independent of temperature for liquid systems, the heat capacity at constant pressure can be calculated. A correction of 6 kcal mol^{-1}K^{-1} has been suggested to be deducted from the heat capacity, which is obtained from energy fluctuations of a classical flexible model [34]. This correction is employed to compensate for the error due to the intra- and intermolecular vibrations compared to a quantum oscillator model [19]. We subtracted the quantum corrections for the high-frequency vibrational modes at different temperatures [68] to calculate the heat capacity in this study.

We calculated the heat capacity via the differentiation of total energy with respect to temperature. The heat capacity at 298 K and 1 atm for water is computed to be 18.75 cal mol^{-1}K^{-1} which is 0.75 cal mol^{-1}K^{-1} greater than the experimental value of 18.00 cal mol^{-1}K^{-1}. The values for heat capacity calculated with AMOEBA14 and AMOEBA03 are 20.48 and 22.36 cal mol^{-1}K^{-1}, respectively [33]. In the AMOEBA14 model, the heat capacity has also been used as data for the parametrization in ForceBalance [33]. In contrast, in this study, we only fitted the parameters to reproduce the experimental heat of vaporization and density at 298 K. Figure 7 shows the experimental and calculated heat capacity in the range of 250–370 K. The MAD from experiment for heat capacity calculated across all temperatures is 1.54 cal mol^{-1}K^{-1} using AMOEBA/GEM-DM, which is lower than the MAD value using AMOEBA14 (2.28 cal mol^{-1}K^{-1}) (see Table 3).

3.2.4 Self-diffusion coefficients

Another liquid property that can be used to validate the quality of the force fields is the self-diffusion coefficient.

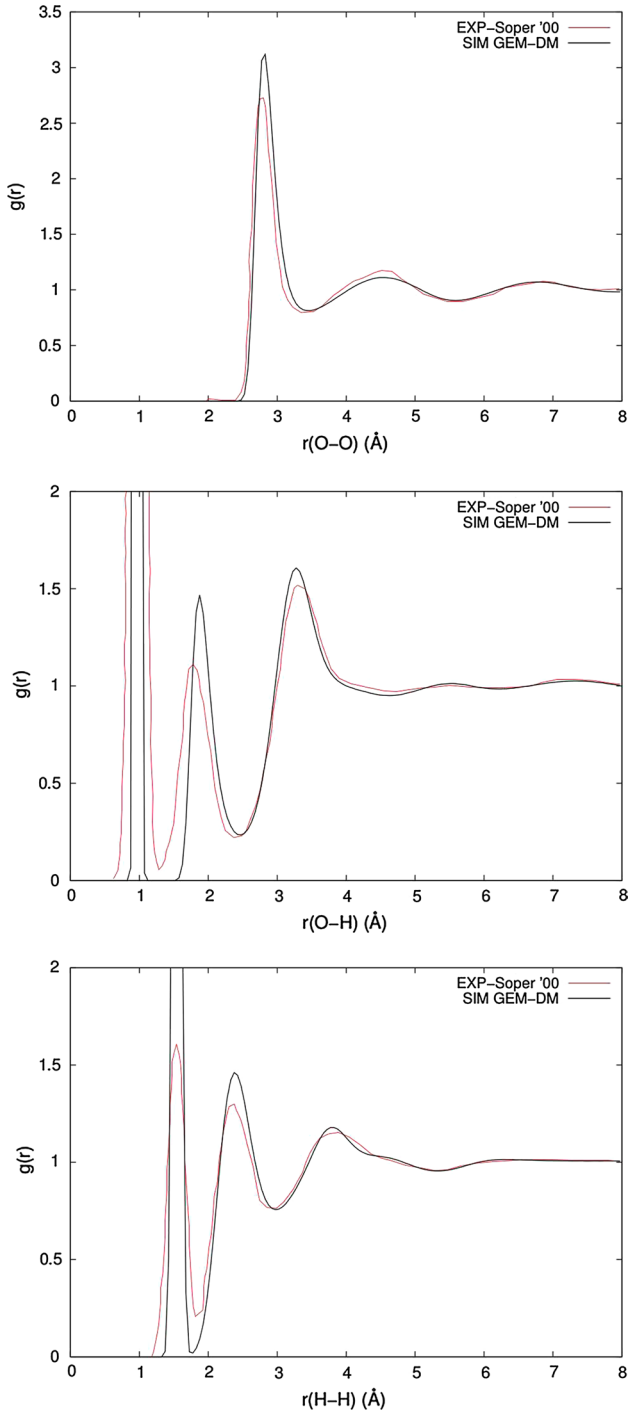

Fig. 9 Radial distribution function for water

The self-diffusion coefficients were calculated using the Einstein relation [1].

$$D_{\pm} = \lim_{t\to\infty} \frac{\langle \mathrm{MSD}(t)_{\pm} \rangle}{6t} \tag{8}$$

where $\langle \mathrm{MSD}(t) \rangle$ is the mean square displacement of the molecule's center of mass and t is the time. The mean square displacement (MSD(t)) in the diffusive regime was calculated from the production trajectories (the last 1.5 ns). Self-diffusion coefficients for the water molecules using AMOEBA/GEM-DM at 298 K are $1.91 \times 10^{-5}\mathrm{cm}^2 s^{-1}$, which is slightly lower than experimental data ($2.29 \times 10^{-5}\mathrm{cm}^2 s^{-1}$). By comparison, the diffusion coefficients calculated with AMOEBA and iAMOEBA are $2 \times 10^{-5}\mathrm{cm}^2 s^{-1}$ and $2.54 \times 10^{-5}\mathrm{cm}^2 s^{-1}$ [49, 68]. The calculated diffusion coefficients for temperatures between 250 and 370 K are shown and compared to available experimental data in Fig. 8. The trend in the self-diffusion coefficients is well correlated with the enthalpies of vaporization. At higher temperature, the present model predicts faster diffusion rate and lower heat of vaporization.

3.2.5 Intermolecular structure

The liquid structure of water is usually described by radial distribution functions (RDFs). These data can be compared to experimental neutron diffraction data [54]. The calculated oxygen–oxygen, oxygen–hydrogen, and hydrogen–hydrogen RDFs and experimental data are depicted in Fig. 9. AMOEBA/GEM-DM model is in good agreement with experimental data for all RDFs. The first peak for the oxygen–oxygen RDF is located at the same distance as experiment (2.8 Å) with a height of 3.12, which is slightly higher than experimental value 2.73. The second peak, as well as the first and second troughs of the oxygen–oxygen RDF, is in excellent agreement with experiment. RDFs for oxygen–hydrogen and hydrogen–hydrogen show similar level of agreement.

4 Conclusions

We have presented a new AMOEBA polarizable model for water that uses GEM distributed multipoles with higher-order multipoles on the oxygen and hydrogen atoms. The new parameters improved accuracy for several properties, including ρ, ΔH_{vap}, C_p and D for a range of temperatures compared to our previous parameters. This improvement is mainly due to the inclusion of dipoles and quadrupoles on the hydrogen atoms, which provides a better description of polarization and electrostatics. Although we only adjusted the van der Waals parameters to reproduce the experimental density and heat of vaporization at 298 K, the model shows very good agreement for a series of thermodynamic properties including density, heat of vaporization, heat capacity, and diffusion coefficient for a range of temperatures. Mean absolute deviations calculated for density, heat of vaporization, and heat capacity confirm the excellent agreement between experimental data and simulation results in the range of 250–370 K.

Acknowledgments This work was supported by Wayne State University. Computing time from Wayne State's C&IT is gratefully acknowledged.

References

1. Allen MP, Tildesley DJ (1987) Computer simulation of liquids. Clarendon Press, Oxford
2. Andzelm J, Wimmer E (1992) Density functional gaussian-type-orbital approach to molecular geometries, vibrations and reaction energies. J Chem Phys 96:1280–1303
3. Babin V, Leforestier C, Paesani F (2013) Development of a "first principles" water potential with flexible monomers: dimer potential energy surface, VRT spectrum, and second virial coefficient. J Chem Theory Comput 9(12):5395–5403
4. Babin V, Medders GR, Paesani F (2014) Development of a "first principles" water potential with flexible monomers. II: trimer potential energy surface, third virial coefficient, and small clusters. J Chem Theory Comput 10(4):1599–1607
5. Barnes P, Finney J, Nicholas J, Quinn J (1979) Cooperative effects in simulated water. Nature 282:459–464
6. Boys SF, Bernardi Fd (1970) The calculation of small molecular interactions by the differences of separate total energies. Some procedures with reduced errors. Mol Phys 19(4):553–566
7. Burger SK, Cisneros GA (2013) Efficient optimization of van der waals parameters from bulk properties. J Comput Chem 34(27):2313–2319
8. Caldwell J, Dang LX, Kollman PA (1990) Implementation of nonadditive intermolecular potentials by use of molecular dynamics: development of a water-water potential and water-ion cluster interactions. J Am Chem Soc 112(25):9144–9147
9. Caldwell JW, Kollman PA (1995) Structure and properties of neat liquids using nonadditive molecular dynamics: water, methanol, and n-methylacetamide. J Phys Chem 99(16):6208–6219
10. Case D, Darden T, Cheatham T III, Simmerling C, Wang J, Duke R, Luo R, Walker R, Zhang W, Merz K et al (2012) Amber 12. University of California. San Francisco 1(2):3
11. Cisneros GA (2012) Application of gaussian electrostatic model (GEM) distributed multipoles in the AMOEBA force field. J Chem Theory Comput 8(12):5072–5080
12. Cisneros GA, Piquemal JP, Darden TA (2005) Intermolecular electrostatic energies using density fitting. J Chem Phys 123:044109
13. Cisneros GA, Piquemal JP, Darden TA (2006) Generalization of the gaussian electrostatic model: extension to arbitrary angular momentum, distributed multipoles and computational speedup with reciprocal space methods. J Chem Phys 125:184101
14. Cisneros GA, Tholander SNI, Parisel O, Darden TA, Elking D, Perera L, Piquemal JP (2008) Simple formulas for improved point-charge electrostatics in classical force fields and hybrid quantum mechanical/molecular mechanical embedding. Int J Quantum Chem 108:1905–1912
15. Corongiu G, Clementi E (1992) Erratum: liquid water with an abinitio potential: X-ray and neutron scattering from 238 to 368 k. J Chem Phys 97(11):8818–8818 J Chem Phys 97:2030 (1992)
16. Darden TA, York D, Pedersen LG (1993) Particle mesh Ewald: an nlog(n) method for Ewald sums. J Chem Phys 98:10089–10092
17. Day PN, Jensen JH, Gordon MS, Webb SP, Stevens WJ, Krauss M, Garmer D, Basch H, Cohen D (1996) An effective fragment method for modeling solvent effects in quantum mechanical calculations. J Chem Phys 105:1968–1986
18. Duke RE, Starovoytov ON, Piquemal JP, Cisneros GA (2014) GEM*: a molecular electronic density-based force field for molecular dynamics simulations. J Chem Theory Comput 10(4):1361–1365
19. Eisenberg D, Kauzmann W (1969) The structure and properties of water. Oxford University Press, London
20. Essmann U, Perera L, Berkowitz M, Darden TA, Lee H, Pedersen LG (1995) A smooth particle mesh Ewald method. J Chem Phys 103:8577–8593
21. Freitag MA, Gordon MS, Jensen JH, Stevens WJ (2000) Evaluation of charge penetration between distributed multipolar expansions. J Chem Phys 112:7300–7306
22. Fuentes-Azcatl R, Alejandre J (2014) Non-polarizable force field of water based on the dielectric constant: Tip4p/ε. J Phys Chem B 118(5):1263–1272
23. Gresh N, Cisneros GA, Darden TA, Piquemal JP (2007) Anisotropic, polarizable molecular mechanics studies of inter- and intramolecular interactions and ligand-macromolecule complexes. A bottom-up strategy. J Chem Theory Comput 3(6):1960–1986
24. Guillot B (2002) A reappraisal of what we have learnt during three decades of computer simulations on water. J Mol Liquids 101(1):219–260
25. Halgren TA (1992) The representation of van der waals (vdw) interactions in molecular mechanics force fields: potential form, combination rules, and vdw parameters. J Am Chem Soc 114(20):7827–7843
26. Halgren TA, Damm W (2001) Polarizable force fields. Curr Opin Struct Biol 11(2):236–242
27. Hermida-Ramón JM, Brdarski S, Karlström G, Berg U (2003) setminusinter-and intramolecular potential for the n-formylglycinamide-water system. A comparison between theoretical modeling and empirical force fields. J Comput Chem 24(2):161–176
28. Jorgensen WL, Chandrasekhar J, Madura JD, Impey RW, Klein ML (1983) Comparison of simple potential functions for simulating liquid water. J Chem Phys 79(2):926–935
29. Kairys V, Jensen JH (1999) Evaluation of the charge penetration energy between non-orthogonal molecular orbitals using the spherical gaussian overlap approximation. Chem Phys Lett 315(1–2):140–144
30. Kiss PT, Bertsyk P, Baranyai A (2012) Testing recent charge-on-spring type polarizable water models. I. Melting temperature and ice properties. J Chem Phys 137(19):194102
31. Kitaura K, Morokuma K (1976) A new energy decomposition scheme for molecular interactions within the Hartree-Fock approximation. Int J Quantum Chem 10(2):325–340
32. Kosov D, Popelier P (2000) Atomic partitioning of molecular electrostatic potentials. J Phys Chem A 104(31):7339–7345
33. Laury ML, Wang LP, Pande VS, Head-Gordon T, Ponder JW (2015) Revised parameters for the amoeba polarizable atomic multipole water model. J Phys Chem B 119(29):9423–9437
34. Levitt M, Hirshberg M, Sharon R, Laidig KE, Daggett V (1997) Calibration and testing of a water model for simulation of the molecular dynamics of proteins and nucleic acids in solution. J Phys Chem B 101(25):5051–5061
35. Mark P, Nilsson L (2001) Structure and dynamics of the tip3p, spc, and spc/e water models at 298 K. J Phys Chem A 105(43):9954–9960
36. Medders GR, Babin V, Paesani F (2014) Development of a "first-principles" water potential with flexible monomers. III. Liquid phase properties. J Chem Theory Comput 10(8):2906–2910
37. Nam K, Gao J, York DM (2005) An efficient linear-scaling ewald method for long-range electrostatic interactions in combined qm/mm calculations. J Chem Theory Comput 1:2–13
38. Narten A, Levy H (1971) Liquid water: molecular correlation functions from X-ray diffraction. J Chem Phys 55(5):2263–2269
39. Neilson G, Enderby J (1996) Aqueous solutions and neutron scattering. J Phys Chem 100(4):1317–1322
40. Neilson GW, Enderby JE (1986) Water and aqueous solutions: proceedings of the thirty-seventh symposium of the Colston

Research Society, held in the University of Bristol in April 1985, vol 37. Taylor & Francis, New York
41. Paesani F, Voth GA (2009) The properties of water: insights from quantum simulations. J Phys Chem B 113(17):5702–5719
42. Piquemal JP, Cisneros GA, Reinhardt P, Gresh N, Darden TA (2006) Towards a force field based on density fitting. J Chem Phys 124:104101
43. Piquemal JP, Gresh N, Giessner-Prettre C (2003) Improved formulas for the calculation of the electrostatic contribution to the intermolecular interaction energy from multipolar expansion of the electronic distribution. J Phys Chem A 107:10353–10359
44. Ponder JW, Wu C, Ren P, Pande VS, Chodera JD, Schnieders MJ, Haque I, Mobley DL, Lambrecht DS, Robert A, Jr DiStasio, Head-Gordon M, Clark GNI, Johnson ME, Head-Gordon TJ (2010) Current status of the AMOEBA polarizable force field. J Phys Chem B 114:2549–2564
45. Popelier P, Joubert L, Kosov D (2001) Convergence of the electrostatic interaction based on topological atoms. J Phys Chem A 105(35):8254–8261
46. Popelier P, Kosov D (2001) Atom–atom partitioning of intramolecular and intermolecular coulomb energy. J Chem Phys 114(15):6539–6547
47. Popelier PL, Hall P (2000) Atoms in molecules: an introduction. Prentice Hall, London
48. Ren P, Ponder JW (2002) Consistent treatment of inter-and intramolecular polarization in molecular mechanics calculations. J Comput Chem 23(16):1497–1506
49. Ren P, Ponder JW (2003) Polarizable atomic multipole water model for molecular mechanics simulation. J Phys Chem B 107(24):5933–5947
50. Ren P, Ponder JW (2004) Temperature and pressure dependence of the amoeba water model. J Phys Chem B 108(35):13427–13437
51. Ren P, Wu C, Ponder JW (2011) Polarizable atomic multipole-based molecular mechanics for organic molecules. J Chem Theory Comput 7(10):3143–3161
52. Rick SW, Stuart SJ (2002) Potentials and algorithms for incorporating polarizability in computer simulations. Rev Comput Chem 18:89–146
53. Sellberg JA, Huang C, McQueen T, Loh N, Laksmono H, Schlesinger D, Sierra R, Nordlund D, Hampton C, Starodub D et al (2014) Ultrafast X-ray probing of water structure below the homogeneous ice nucleation temperature. Nature 510(7505):381–384
54. Soper A (2000) The radial distribution functions of water and ice from 220 to 673 k and at pressures up to 400 mpa. Chem Phys 258(2–3):121–137
55. Sorenson JM, Hura G, Glaeser RM, Head-Gordon T (2000) What can X-ray scattering tell us about the radial distribution functions of water? J Chem Phys 113(20):9149–9161
56. Starovoytov ON, Torabifard H, Cisneros GA (2014) Development of amoeba force field for 1, 3-dimethylimidazolium based ionic liquids. J Phys Chem B 118(25):7156–7166
57. Stevens WJ, Fink WH (1987) Frozen fragment reduced variational space analysis of hydrogen bonding interactions. Application to the water dimer. Chem Phys Lett 139(1):15–22
58. Stone AJ (1981) Distributed multipole analysis, or how to describe a molecular charge distribution. Chem Phys Lett 83:233–239
59. Stone AJ (2000) The theory of intermolecular forces. Oxford University Press, Oxford
60. Stone AJ (2011) Electrostatic damping functions and the penetration energy. J Phys Chem A 115(25):7017–7027
61. Thole B (1981) Molecular polarizabilities calculated with a modified dipole interaction. Chem Phys 59:341–350
62. Thole BT (1981) Molecular polarizabilities calculated with a modified dipole interaction. Chem Phys 59(3):341–350
63. Vega C, Abascal JL (2011) Simulating water with rigid non-polarizable models: a general perspective. Phys Chem Chem Phys 13(44):19663–19688
64. Vega C, Abascal JL, Conde M, Aragones J (2009) What ice can teach us about water interactions: a critical comparison of the performance of different water models. Faraday Discuss 141:251–276
65. Vega C, Sanz E, Abascal J (2005) The melting temperature of the most common models of water. J Chem Phys 122(11):114507–114507
66. Wang B, Truhlar DG (2010) Including charge penetration effects in molecular modeling. J Chem Theory Comput 6(11):3330–3342
67. Wang L-P. ForceBalance: systematic force field optimization. https://simtk.org/home/forcebalance/. Accessed 24 March 2013
68. Wang LP, Head-Gordon TL, Ponder JW, Ren P, Chodera JD, Eastman PK, Martí-nez TJ, Pande VS (2013) Systematic improvement of a classical molecular model of water. J Phys Chem B. doi:10.1021/jp403802c
69. Xie W, Gao J (2007) Design of a next generation force field: the x-pol potential. J Chem Theory Comput 3(6):1890–1900
70. Xie W, Orozco M, Truhlar DG, Gao J (2009) X-pol potential: an electronic structure-based force field for molecular dynamics simulation of a solvated protein in water. J Chem Theory Comput 5(3):459–467